Infrastructure Assessment with Small Unmanned Aircraft Systems

James V. Henrickson, Cameron Rogers,
Han-Hsun Lu, John Valasek
Department of Aerospace Engineering
Texas A&M University
College Station, Texas 77843
Email: {james.henrickson, crogers, hanhsun.lu, valasek}@tamu.edu

Yeyin Shi
Department of Biological and Agricultural Engineering
Texas A&M University
College Station, Texas 77843
Email: yeyin.shi@tamu.edu

Abstract—As small unmanned aircraft systems become increasingly affordable, reliable, and formally recognized under federal regulation, they become increasingly attractive as novel platforms for civil applications. This paper details the development and demonstration of both fixed-wing and rotorcraft-based unmanned systems for infrastructure assessment tasks. Tasks such as inspecting pavement condition and vegetation encroachment on roadways, debris and tree coverage on railways, and corrosion on bridges and water towers are considered. Rationale for sensor, vehicle, and ground equipment selections are provided, in addition to developed flight operation procedures for two-man crews. Preliminary imagery results are presented and analyzed, and these results demonstrate that both fixed-wing and rotor-wing small unmanned aircraft systems hold promise in enabling rapid and cost-efficient infrastructure health assessment.

I. INTRODUCTION

As commercial unmanned aircraft system (UAS) hardware becomes increasingly affordable and reliable, interest in applying these technologies to novel areas has steadily increased. In recent years, action based on this interest has been impeded by the realities of federal airspace regulation. Commercial usage of UAS in particular has been restricted by the Federal Aviation Administration (FAA) to rare instances that are approved through a costly and time-consuming process on a case-by-case basis. Recently proposed FAA regulation changes, however, promise to open the door to more widespread commercial use of UAS.

A growing area of interest for UAS application is infrastructure assessment. Periodic inspection and assessment of roads, railroads, pipelines, bridges, etc., is currently a costly and time-consuming endeavor. It in many cases requires large teams of trained workers operating specialized machinery that is costly to set up and operate. The challenge of maintaining infrastructure health in the US will only continue to grow in importance over the coming years. The severity of failing to rise to this challenge is illustrated by the 2005 levee failures in New Orleans, Louisiana, caused by Hurricane Katrina, the 2007 I-35W Mississippi River bridge collapse in Minnesota, and the 2005 Taum Sauk Hydroelectric Power Station upper reservoir failure in Missouri. Infrastructure assessment is and will continue to be of the utmost importance, and UAS stand to serve as novel tools for this purpose that lower costs and greatly facilitate the collection of high quality imagery data focused on assessing infrastructure health.

UAS have been shown to be useful tools providing high performance and cost-effective solutions in a diverse range of areas. A 2012 survey of UAS applications found UAS to be reliable platforms for research and civil missions [1]. Ristorto et al. [2] used UAS as a flexible crop management tool demonstrated by the ease of changing between multiple sensor packages. Schwarzbach et al. [3] successfully implemented UAS for sampling water of remote wetland ecosystems. In urban environments, UAS were shown to be a cost-effective and flexible platform for traffic monitoring by Kanistras et al. [4]. Other explored UAS applications have included real-time river flooding assessment [5], river mapping for water management [6], [7], and rangeland surveillance [8].

Infrastructure assessment with UAS is an area in which many specific missions have been studied [9]–[12]. Larrauri et al. used UAS to detect vegetation encroachment into overhead power lines. Roper et al. also investigated the feasibility of UAS in a survey of remote sensing platforms to detect vegetation encroachment on pipelines. Dobson et al. studied the use of UAS for creating 3D models of unpaved roads in order to assess damage and maintenance needs. Additionally, many have investigated the use of UAS in the evaluation of transportation infrastructure, civil service facilities, and telecommunication services in disaster scenarios [13]–[15]. In contrast to the cited examples, which investigate specific mission feasibility, this paper examines the feasibility of using small UAS to conduct a broad range of infrastructure assessment missions using low cost UAS, autopilots, and sensors. Cost and mission flexibility are key factors for expanding UAS operations for infrastructure assessment into larger entities such as local and state governments.

The Texas A&M Transportation Institute (TTI) has recently initiated research focused on demonstrating and assessing UAS infrastructure assessment capabilities using both fixed-wing

and rotorcraft-based platforms. This work is being conducted by the Texas A&M Vehicle Systems and Control Laboratory (VSCL). The specific objectives of this work are to develop methodologies and procedures for infrastructure assessment, assess performance of sensor and vehicle platforms in a variety of real-world infrastructure assessment scenarios, and to develop and demonstrate recommended training and operational procedures for small crew infrastructure assessment data collection operations.

This paper is organized as follows: Section II describes the selected sensors, vehicle platforms (both fixed-wing and rotorcraft), and ground equipment, as well as providing justification for these selections in the context of infrastructure assessment demonstration. Section III details the developed procedures for operating these systems for infrastructure assessment purposes. Section IV provides some example images and performance assessments of the tested hardware and procedures. Sections V and VI provide some concluding thoughts and describe current plans for continuation of this work.

II. Flight Hardware

Hardware was largely selected based on the extensive prior experience of the VSCL in operating UAS. In areas relatively lacking in prior experience, a systems engineering based exercise was conducted to identify and evaluate multiple options for selecting, assessing, and comparing sensors and systems. With a goal of demonstrating infrastructure assessment data collection capabilities, hardware selection was driven by an initial selection of image sensors. Based on the payload requirements derived from these sensors, appropriate fixed-wing and rotorcraft vehicle platforms were selected, and required ground equipment was then identified based on the operational needs of the selected sensor and vehicle systems.

A. Sensors

Three primary sensors were selected for testing and demonstration purposes. The first is a Sentek GEMS Multispectral Sensor (Figure 1), a light-weight stand-alone unit with dual 1.3-megapixel (MP) CMOS sensors for visual (RGB) and near infrared (NIR) imagery collection that costs approximately $1500. The unit weighs 0.57 lbs, has dimensions of $3.5 \times 5.0 \times 2.0$ inches, and has a built in inertial navigation system (INS) and GPS antenna. When set to 1.3-MP images, the Sentek sensor is capable of recording an image (both RGB and NIR) once every 1.4 seconds. The decision to include a multispectral sensor in this project was driven by interest in scenarios in which infrastructure health can be correlated to vegetation—e.g., identifying oil pipeline or irrigation leaks by assessing adjacent vegetation patterns, or locating areas of deteriorating road or railway health by identifying encroaching vegetation. This particular multispectral sensor was selected based on extensive prior experience in operating multispectral sensors in the context of a precision agriculture research project, in which a number of crop fields were periodically surveyed with UAS by the VSCL. The Sentek sensor, in comparison with other tested multispectral sensors, proved to

Fig. 1: Sentek GEMS Multispectral Sensor (with and without Outer Case)

be the most reliable and user-friendly, and achieved the most consistently high quality imagery data.

The second selected sensor is a Canon EOS 5D Mark III DSLR camera (Figure 2). This Canon DSLR has a 22.3-MP CMOS sensor for RGB imagery and costs $3500. Selected with this sensor was a 24-105mm f/4 lens and a Marrex MX-G10 external GPS antenna. The unit weighs 3.2 lbs and has dimensions of $6.0 \times 4.6 \times 6.0$ inches. When set to 22.3-MP, this sensor is capable of recording images at approximately 10 Hz. Whereas the multispectral sensor was selected for senario in which infrastructure health can be indirectly assessed by observing its surroundings, this sensor was selected for instances in which health assessment must be made using direct observations—e.g., inspecting the underside of a bridge or overpass. For these scenarios, in which detailed imagery of the structure itself is more desirable than area coverage over several spectra, a much higher resolution sensor is desirable. Compared with the 1.3-MP Sentek sensor, the 22.3-MP Canon camera is capable of acquiring higher resolution imagery in the visual spectrum. This specific camera was selected based on past experience with operating a similar Nikon DSLR camera on the aforementioned precision agriculture project.

The final sensor selected for testing is a GoPro HERO3+ Silver Edition. This GoPro sensor is capable of recording high-definition $1920 \times 1080p$ RGB video imagery at 60 frames per second, weighs 2.6 ounces, and has dimensions of $2.3 \times 1.6 \times 1.2$ inches. Unlike the Sentek multispectral sensor and Canon DSLR camera, which were selected for (whether directly or indirectly) assessing infrastructure health, this GoPro sensor was selected for situational awareness purposes. Particularly

Fig. 2: Canon EOS 5D Mark III DSLR Camera and External GPS Antenna

Fig. 3: ReadyMadeRC Anaconda Vehicle

Fig. 4: Hangar 9 1/4-Scale Super Cub Vehicle

when operating UAS in spaces with obstacles and obstructions, such as around a bridge or overpass, it is crucial that the operators maintain the ability to perceive the environment immediately surrounding the vehicle to avoid collisions. GoPro cameras, being small and lightweight, are well-suited for providing live video from UAS to system operators on the ground. Though useful for live video monitoring, a limitation of the GoPro camera is that it does not include nor easily support the use of a GPS module; as such, images taken cannot be geo-tagged for post-flight mosaicking.

B. Fixed-wing Systems

Vehicle airframe selection was driven by sensor selection. For scenarios in which it is desirable to cover large areas or distances, vehicle endurance and range become critical factors. For these scenarios, such as a vehicle imaging several miles of oil pipeline or railway, fixed-wing vehicles are preferable. With these scenarios in mind, two fixed-wing vehicles were selected for testing.

1) Anaconda: The first selected fixed-wing vehicle is the ReadyMadeRC Anaconda (Figure 3). An Anaconda airframe has an empty weight of 5.3 pounds, a wingspan of 6.8 feet, and can carry a payload of 4 pounds for 45-60 minutes. Originally intended for first-person view (FPV) hobbyists, an Anaconda airframe costs roughly $400 and is designed to easily accommodate sensors in its fuselage. Out of the box, the airframe includes mounting brackets for installing a GoPro camera in either a fixed position looking forward, or on a gimbal mount hanging underneath nose. The Anaconda airframe was selected primarily for its low-cost, its durable foam construction, and its relatively large and easily accessible sensor payload area. Anaconda was the airframe of choice for VSCL precision agriculture research data collection in 2015, in which over 60 flights were conducted over the course of four months. This previous experience made Anaconda the natural first choice for a fixed-wing platform for infrastructure assessment. The Anaconda for this project has been equipped with the Sentek multispectral sensor—mounted looking downward in a fixed position beneath the wing.

2) Super Cub: Requiring a larger fixed-wing airframe to accommodate the Canon DSLR camera, the second fixed-wing airframe selected is the Hangar 9 1/4-Scale Super Cub (Figure 4). With an empty weight of 16.6 pounds, a wingspan of 8.8

feet, the $1200 Super Cub airframe is larger than Anaconda, and is capable of carrying a 10 pound payload for 30-40 minutes. Although not specifically intended for carrying sensor payloads, this airframe was selected for its payload carrying capacity, its favorable low-speed handling qualities, and its suitability for rough field takeoffs and landings.

C. Rotorcraft Systems

It was decided in the early stages of this project that fixed-wing and rotorcraft vehicles are well suited for different domains of infrastructure assessment. Rather than limiting the scope of the project to one of these domains, it was decided that vehicles of both types would be selected to demonstrate capabilities in as wide of a range of scenarios as possible. As described, fixed-wing platforms are well-suited for scenarios requiring endurance and coverage. Rotorcraft, however, are well-suited for scenarios in which obtaining *detailed* imagery is more crucial, and for scenarios that require data collection in areas that are otherwise inaccessible by typical fixed-wing vehicles.

1) DJI S1000+ Octocopter: Intended to carry the Canon DSLR camera, the DJI S1000+ octocopter (Figure 5) was selected as the primary rotorcraft airframe for this project. With an empty weight of 9 pounds and a diagonal wheelbase of 3.6 feet, the S1000 is capable of carrying 12 pounds for

Fig. 5: DJI S1000+ Octocopter Vehicle

Fig. 7: IntelinAir RD-100 Hexacopter

Fig. 6: DSLR 3-Axis Gimbal Mount

D. Avionics

In terms of avionics, beyond the standard hobbyist radio controlled (R/C) electronics (receiver, electronic speed control, servos, etc), two autopilots have been used on vehicles as a part of this project.

1) Pixhawk: The primary autopilot used by the VSCL is the Pixhawk, a $300 commercially available hobby-grade autopilot that includes INS and GPS sensors, is easily configurable for standard R/C airframes, and supports firmware for both fixed-wing (ArduPlane) and rotorcraft (ArduRotor). This autopilot provides several basic flight modes including waypoint navigation, in which the vehicle autonomously follows a specified mission profile, and a variety of stability augmentation modes. For a fixed-wing vehicle, for instance, a "stabilize" mode will cause the vehicle to return to wings-level flight when the pilot is not providing input controls. For a rotorcraft, a similar "position hold" mode has the vehicle hover in place when not being manually controlled. Additionally, this autopilot allows vehicle operators to set failsafe behaviors, interface with camera gimbals onboard the vehicle, and view and log vehicle telemetry while the vehicle is in flight. Pixhawks have been the primary autopilot used by the VSCL since early 2014 and as such were the logical starting point as a primary avionics package for this project. Pixhawks are currently installed on all previously-mentioned vehicles with the exception of the IntelinAir RD-100 hexacopter.

2) IntelinAir SafeSmart: While the Pixhawk autopilot provides basic functionality at an affordable price point that is relatively easy to configure, it is ill-suited for custom control algorithm implementation. Particularly interested in opening up the possibility of developing custom controls for intelligent obstacle avoidance with rotorcraft, the VSCL elected to investigate a more research-grade autopilot that would be better suited to the implementation of custom control algorithms. The IntelinAir SafeSmart autopilot (seen as the red module in the center of Figure 8) was selected for this purpose. The IntelinAir autopilot is roughly a $1000 unit that provides much

roughly 12-15 minutes. This airframe was selected based on its carrying capacity—in terms of both mass and volume as the frame can accommodate the Canon DSLR camera with a 3-axis gimbal mount. This gimbal mount will both stabilize the camera and allow for a ground operator to control the orientation of the camera with respect to the vehicle while the it is in flight.

2) Hexcopter: For scenarios that require close inspection of infrastructure without necessarily requiring the full resolution provided by the Canon DSLR camera, a smaller hexacopter was selected that is capable of carying a GoPro camera in either a fixed mount or gimbal mount configuration. The airframe selected for this purpose was the IntelinAir RD-100 (Figure 7), a modified DJI Flame Wheel F550. The IntelinAir hexacopter has an empty weight of 1.1 pounds, a diagonal wheelbase of 1.8 feet, and can carry a 3 pound payload for 12-15 minutes. It was selected for two reasons. First, it is smaller and more portable than the S1000 octocopter while still capable of easily carrying a GoPro with gimbal mount. Second, the IntelinAir RD-100 is packaged with a unique autopilot, described below, that is designed to facilitate custom control algorithm implementation.
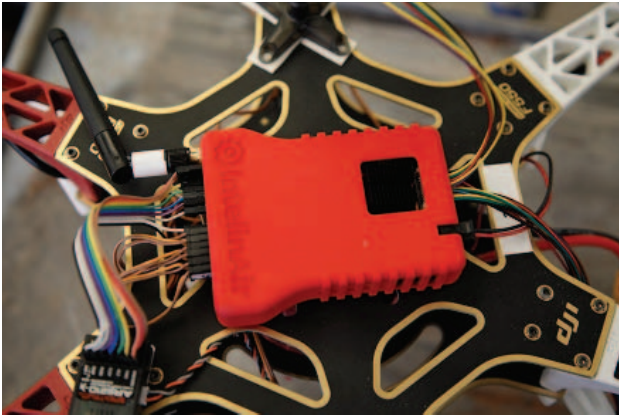
Fig. 8: IntelinAir SafeSmart Autopilot

of the same functionality as the Pixhawk autopilot (though currently limited to exclusively rotorcraft vehicles). Unlike Pixhawk, however, the IntelinAir autopilot supports direct implementation of custom control algorithms synthesized with Simulink.

E. Ground Equipment

Supporting ground equipment required to conduct flight operations is essentially identical for both fixed-wing and rotorcraft flights. Both scenarios require a ground control station notebook computer, a telemetry radio, an R/C transmitter, flight batteries, and a few simple tools (screwdriver, pliers, etc). Portability and durability were two areas of priority in creating an equipment checklist for infrastructure assessment UAS flight operations. To satisfy the durability requirement, a Panasonic Toughbook (Figure 9) was selected to serve as the ground control station. This machine, which weighs approximately 8 pounds and has an 18-hour battery life, has been equipped with APM Mission Planner, the software used in junction with Pixhawk autopilots. Mission Planner allows one to create and save mission plans, monitor vehicle telemetry, and otherwise communicate with the vehicle. To communicate with the IntelinAir autopilot installed on the RD-100 hexacopter, a separate piece of software, IntelinAir AirStation, is also installed on this machine. AirStation essentially performs the same functionality as Mission Planner, but it is specific to the IntelinAir SafeSmart autopilot. All flight hardware, minus the vehicle, for both fixed-wing and rotorcraft flights is stored and transported in a rugged Pelican case, shown in Figure 10. This both protects the equipment and allows a two-man team to rapidly relocate between data collection flights.

Fig. 9: Toughbook GCS Running APM Mission Planner

Fig. 10: Ground Equipment in Pelican Case

III. PROCEDURES

A. Fixed-wing System Operation

The advantages of UAS are overt—that is, the capability to take off and land in limited time and space, and the ability to reduce the cost of each survey flight. Fixed-wing UAS especially have the capability of operating missions covering larger survey areas and requiring longer air time. A two-man,

high mobility, easy operational fixed-wing flight procedure is developed to react to missions with short preparation. The two-man crew includes a Ground Control Station (GCS) operator and a pilot. The flight-ready items are an equipped $24 \times 19 \times 9$ inch pelican case and a pre-trimmed fixed-wing UAS. For pre-flight preparation, the two-man crew ensures that the following items are included in the pelican case: an R/C transmitter, a telemetry radio, short-range radios, basic tools (screwdriver,

pliers, etc), a laptop with Mission Planner, and charged flight batteries.

Upon arriving at the observation site, the GCS operator sets up the ground control station in the bed of a pickup truck or the back of an SUV. An example setup is shown in Figure 11. As the GCS operator prepares the ground station, the pilot inspects the takeoff runway, removing any large debris. When operating an Anaconda or Super Cub, the takeoff/landing space should be approximately 200 by 15 feet and unobstructed by adjacent trees, power lines, or other obstacles. Before starting the mission, the two-man crew must decide the survey area of interest and discuss any potential mission difficulties (such as adverse wind conditions, flight path obstacles, possible runway incursions, etc) before further preparation. The pilot is responsible for the readiness of the aircraft, including connecting the batteries and checking servo reactions; the GCS operator is responsible for setting the waypoints and uploading the mission to the autopilot onboard the vehicle. For a typical area survey mission, the first and last waypoints are set as loiter points. The vehicle autonomously circles these designated points before starting and after finishing the survey mission. Loitering before starting the mission allows the crew to examine of the condition of the vehicle and weather before deciding whether to proceed or terminate the mission. Similarly, loitering once the mission is finished allows the crew to wait for favorable wind conditions and clear any runway incursions before landing the vehicle.

While on mission, the pilot is responsible for manually taking off/landing the vehicle, as well as manually controlling the vehicle before handing it off to the autopilot software. After handing control to the autopilot, the primary task for the pilot is to observe the vehicle and re-take manual control in the event of any off-nominal events. Such events may include airspace incursions by other manned or unmanned aircraft or vehicle malfunction. While the pilot visually monitors the UAS during the mission, the GCS operator is responsible for monitoring vehicle telemetry and updating the pilot with mission status information as necessary. The telemetry information of particular interest to the GSC operator is flight mode, current waypoint, altitude, battery health, airspeed, and attitude. Once the mission has been successfully completed, the vehicle will loiter around the last waypoint. The pilot can then re-take manual control and land the vehicle at his or her discretion to end the flight. Note that manual takeoff and landing can both be conducted in a stability augmented flight mode, which significantly reduces the required amount of prior R/C training for the pilot.

This procedure have been rigorously tested. The preparation time once arriving at the observation site is approximately 10 minutes, and the total flying time for the fixed-wing UAS can be up to 40 minutes, which enables missions that can survey up to 100 acres of land in less than an hour.

B. Rotorcraft System Operation

Rotorcraft vehicle operations are similar in many aspects to that of fixed-wing UAS. Upon arrival at the mission site,

Fig. 11: Ground Control Station Setup

the pilot selects an open area for the rotorcraft to perform takeoff and landing. The area selected should be clear of obstacles with sufficient area to accommodate vertical takeoff and landing. The pilot prepares the vehicle by installing avionics and flight batteries. The avionics battery is connected and the GCS operator confirms successful communication between the GCS and vehicle. Together they plan the mission based on assessment objectives and verify that the mission can be completed in under 15 minutes (the typical maximum endurance of the selected rotorcraft vehicles). The GCS operator and pilot then decide, based on weather conditions and equipment status, whether to proceed with or terminate the mission.

The vehicle is sent on mission after the flight battery is connected and the vehicle has been armed by the GCS operator. The pilot performs a takeoff maneuver and manually controls the vehicle to the desired observation positions. The GCS operator is responsible for monitoring the live video feed from the vehicle and controlling the camera gimbal if installed. He verbally communicates to the pilot any vehicle position changes necessary for successful data collection. Additionally, as with fixed-wing vehicle operation, the GCS operator must monitor the state of the vehicle. After completion of the mission, the pilot lands and disarms the UAS.

IV. RESULTS

Several infrastructure assessment demonstration flights have been conducted—primarily with Anaconda airframes. These flights have focused on collecting imagery of a variety of areas of interest located at the Texas A&M Riverside Range ($30°38'22.53''$N, $96°29'3.35''$W), including runway (Figure 12), roads (Figure 13), fields, ponds (Figure 15), wooded terrain, buildings, and oil platforms (Figures 16 and 17). A few imagery result examples are provided here for a series of data collection flights that occurred between October and December 2015 at the Texas A&M Riverside Range.

The objective of these flights was to assess the quality of imagery that could be taken using the Sentek multispectral sensor at a flight altitude of 400 feet and airspeed of approximately 35 miles per hour. Each flight path distance was approximately

half a mile, due to current regulations that require the vehicle to remain in line of sight of the operators, and the paths were generally selected to include a variety of terrain types (paved runway, paved taxiway, grass field, trees, etc). Note that, though in this specific case only half a mile was imaged, vehicle endurance could easily allow for several miles to be imaged in this way in a single flight should FAA regulations relax the line of sight requirement in the future.

Geo-tagged images collected from each flight were mosaicked using Pix4D (Pix4D SA, Lausanne, Switzerland). In order to create mosaics in good quality, the software requires at least 75% of forward-overlap between successive images and 60% of side-overlap between flying tracks. These requirements were achieved with the fixed-wing flights in this project by 1) ensuring the vehicle airspeed was limited to 35 miles per hour, 2) configuring the Sentek multispectral camera at its maximum sampling rate which is 1.4 seconds/frame, and 3) planning dense flying tracks to ensure sufficient side-overlap. Several mosaicked image results of different areas of interest are presented below. With a focal length of 7.7 mm and horizontal and vertical dimensions of the sensors imaging detector of 4.8 and 3.6 mm, respectively, the horizontal and vertical ground coverages of a single image taken by the Sentek multispectral camera at a flight altitude of 400 feet AGL were 250 and 187 feet, respectively. With a pixel resolution of 1280×960, the corresponding ground sampling distance was 2.34 inches.

A. Runway and vegetation areas

Figure 12 shows the results of the flight over runway area conducted on December 3rd, 2015. Healthy vegetation areas appear reddish in the color-infrared map (Figure 12b) and are brighter in the NDVI (normalized difference vegetation index) map (Figure 12c). NDVI is one of the most widely used spectral vegetation indices, which calculates the difference between the near infrared and visible wavelength observations divided by the sum of these measurements [16]. Vegetation areas show much greater NDVI values than non-vegetation areas due to the high spectral reflectance of vegetation in near infrared band. In this study, the NDVI map was used to differentiate vegetation and non-vegetation areas for infrastructure assessment. Figure 13a shows a classified map in which vegetation areas were assigned as green pixels and non-vegetation areas were assigned as gray pixels. Such an analysis can be used to identify areas in which vegetation is encroaching on or penetrating infrastructure such as roads, parking lots, runways, and taxiways. By thresholding the NDVI map, areas can be seen in this figure, for instance, where weeds are growing up through cracks in the runway pavement, highlighted in Figure 13d.

Surface uniformity and condition is also of interest in terms of infrastructure inspection. The blocks on the runway can be easily distinguished from the texture map (Figure 12d), which was the entropy calculated from co-occurrence matrices of each 7 by 7 pixel window of the green spectral band. This can be used, as one example, to identify irregularities and deformities in paved areas. A similar method can also be used

for plant identification purposes [17]. Figure 14 shows the results of the flight along the center runway area conducted on October 8th, 2015. In addition to the aforementioned weed patches, different surface materials of the paved road are clearly shown in both images.
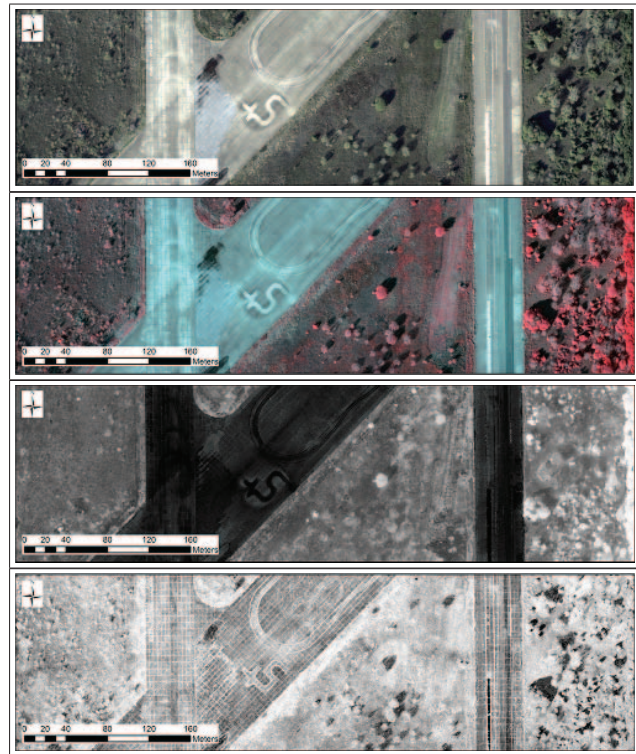

Fig. 12: Runway, paved road and vegetation areas flown on December 3, 2015: (a) RGB map; (b) color-infrared map; (c) NDVI (normalized difference vegetation index) map; (d) texture variation based on entropy measure

B. Pond area

The potential of UAS application in natural resource management was also included in the scope of this study. Figure 15 shows the results of the flight over a pond area conducted on October 15th, 2015. The algae pollution is especially clear in the color-infrared image (Figure 15b).

C. Oil well area

Surface condition is critical to oil well areas to ensure safety during the oil drilling process. Figures 16 and 17 show the results of flights over an oil platform area conducted on November 12th, 2015, and March 2nd, 2016. The sharp color-infrared maps from all flights indicate good alignments between the RGB and NIR bands taken by two different lenses on the Sentek multispectral camera achieved in the post-processing. Similar to the findings from the runway mosaics, some areas with higher near-infrared reflectance inside the paved oil well area were observed in the color-infrared mosaic (Figure 16b) which were corresponding to the higher green pixel values of the RGB mosaic (Figure 16a). An ongoing
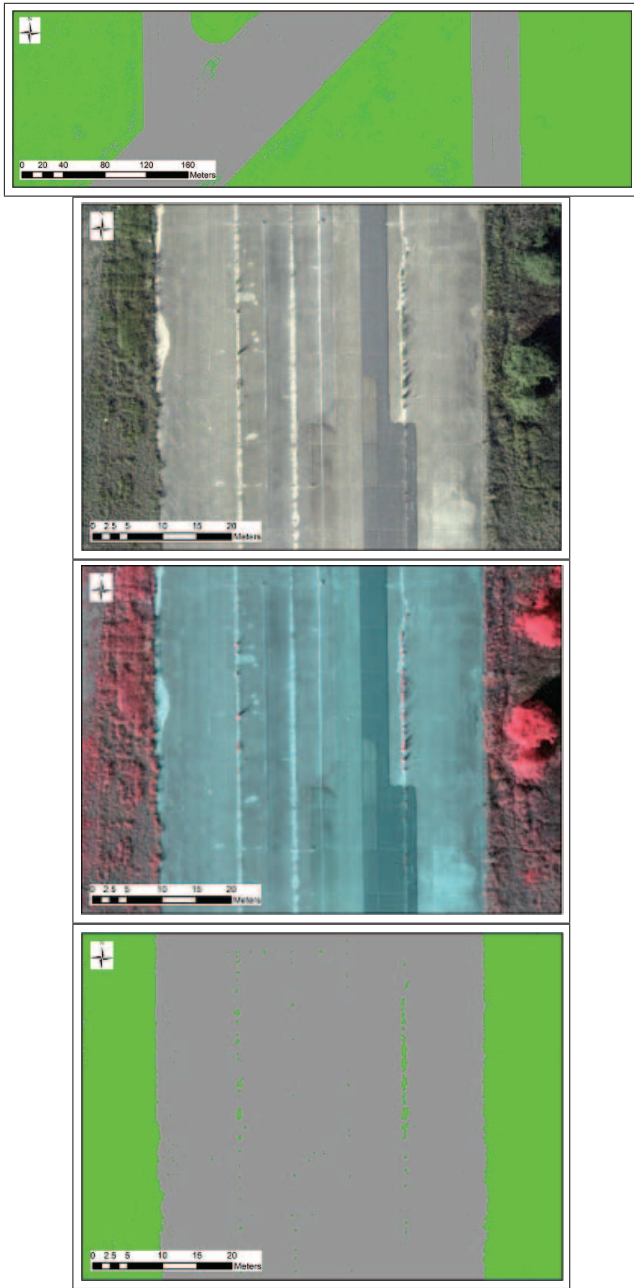
Fig. 13: Classification of vegetation and non-vegetation areas, and weed patch detection on the paved road: (a) classified vegetation (green) and non-vegetation (gray) areas; (b) zoom-in view of RGB map with weed patches; (c) zoom-in view of color-infrared map with weed patches; (d) zoom-in view of classification map showing the detected weed patches in green pixels

study is focused on collecting ground truth surface conditions in the oil well area and comparing against the aerial inspected surface conditions.

Fig. 14: Center runway area flown on October 8th, 2015: (a) RGB map; (b) color-infrared map

V. CONCLUSIONS

A primary objective of this project has been to establish and demonstrate procedures with selected flight hardware that enable a small team to quickly perform infrastructure assessment tasks using UAS. This has been demonstrated with several fixed-wing data collection flights and preliminary rotorcraft testing, using analysis of the collected multi-spectral imagery as the metric. It is clear from this assessment that a two-man crew is capable of operating both fixed-wing and rotorcraft platforms purposed for infrastructure assessment of the tasks addressed by the work in this paper. Additionally, an Anaconda airframe equipped with a Sentek multispectral
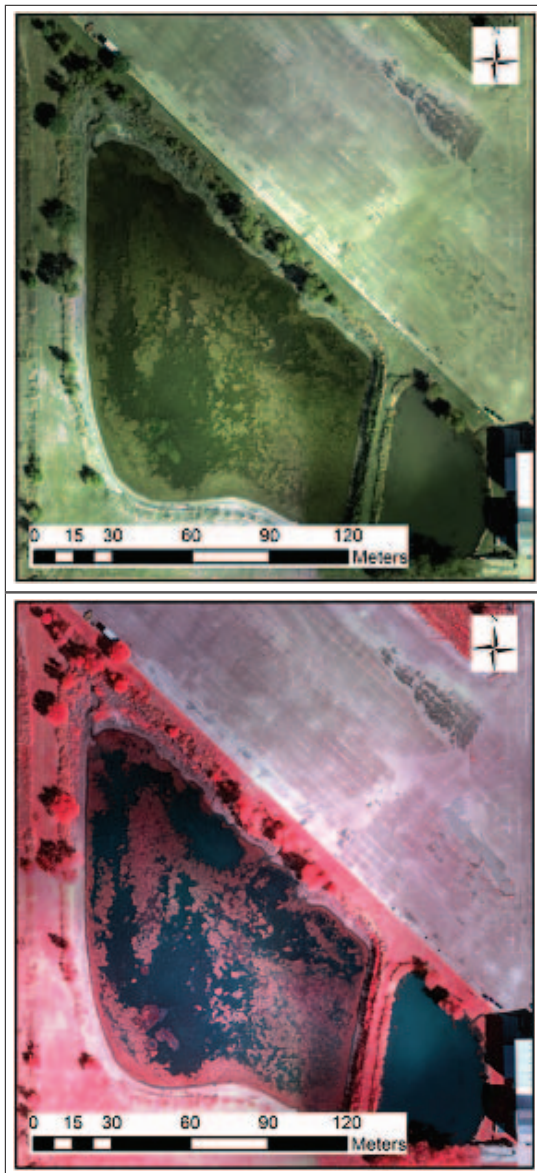
Fig. 15: Pond area flown on October 15th, 2015: (a) RGB map; (b) color-infrared map

Fig. 16: Oil platform area flown on November 12th, 2015: (a) RGB map; (b) color-infrared map

sensor is capable of collecting imagery of sufficient quality for infrastructure assessment purposes. For missions focused on large area surveying, the pairing of a fixed-wing Anaconda vehicle with a multispectral Sentek sensor has demonstrated that a relatively rugged, inexpensive, and easy-to-operate UAS can capture valuable imagery data for infrastructure assessment tasks. Though not yet demonstrated, equally valuable results are expected to be provided with the selected rotorcraft platforms.

VI. FUTURE WORK

Fixed-wing UAS hardware selection and procedures have been sufficiently refined to allow for consistent demonstration of infrastructure assessment flight operations. Future work will include formalizing a set of training documents and procedures

such that a two-man crew can be trained for basic fixed-wing flight operations over the course of one or two business days.

Further refinement of rotorcraft procedures is required before moving onto the development of a rotorcraft training program. The primary point of interest at this stage is addressing situational awareness when operating a rotorcraft vehicle near obstacles. Since rotorcraft vehicles have been selected with the purpose of allowing operators to obtain detailed imagery of overpasses, bridges, water towers, etc, these vehicles will routinely be in close vicinity to potentially dangerous obstacles. Even with a pilot visually monitoring the vehicle at all times, achieving the degree of situational awareness required for safe proximity operations is expected to require additional vehicle-based sensing. Two avenues will be explored in the coming
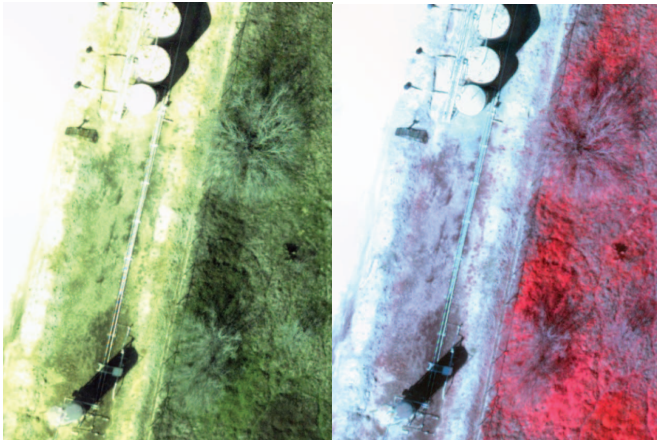
Fig. 17: Oil platform area flown on March 2nd, 2016: (a) RGB map; (b) color-infrared map

months to achieve this task. The first will assess the possibility of using streamed video footage from cameras installed on the vehicle to allow the operators to detect nearby obstacles. Both fixed and gimbaled camera will be tested, as well as multiple display methods (monitor, FPV goggles, etc). The second avenue will involve providing the vehicle itself with sensing and intelligence capabilities to autonomously avoid collision with nearby objects. Sensors tested will include LiDAR, sonar, and possibly RGB cameras coupled with optic flow algorithms. Depending on the reliability of this autonomous approach, some combination of the two approaches may be required to satisfy the desired performance.

REFERENCES

[1] M. Dunbabin and L. Marques, "Robots for environmental monitoring: Significant advancements and applications," *Robotics Automation Magazine, IEEE*, vol. 19, no. 1, pp. 24–39, March 2012.

[2] G. Ristorto, F. Mazzetto, G. Guglieri, and F. Quagliotti, "Monitoring performances and cost estimation of multirotor unmanned aerial systems in precision farming," in *Unmanned Aircraft Systems (ICUAS), 2015 International Conference on*, June 2015, pp. 502–509.

[3] M. Schwarzbach, M. Laiacker, M. Mulero-Pazmany, and K. Kondak, "Remote water sampling using flying robots," in *Unmanned Aircraft Systems (ICUAS), 2014 International Conference on*, May 2014, pp. 72–76.

[4] K. Kanistras, G. Martins, M. Rutherford, and K. Valavanis, "A survey of unmanned aerial vehicles (uavs) for traffic monitoring," in *Unmanned Aircraft Systems (ICUAS), 2013 International Conference on*, May 2013, pp. 221–234.

[5] M. Abdelkader, M. Shaqura, C. Claudel, and W. Gueaieb, "A uav based system for real time flash flood monitoring in desert environments using lagrangian microsensors," in *Unmanned Aircraft Systems (ICUAS), 2013 International Conference on*, May 2013, pp. 25–34.

[6] A. Mancini, E. Frontoni, P. Zingaretti, and S. Longhi, "High-resolution mapping of river and estuary areas by using unmanned aerial and surface platforms," in *Unmanned Aircraft Systems (ICUAS), 2015 International Conference on*, June 2015, pp. 534–542.

[7] M. Schwarzbach, U. Putze, U. Kirchgaessner, and M. v. Schoenermark, "Acquisition of high quality remote sensing data using a uav controlled by an open source autopilot," in *ASME 2009 International Design Engineering Technical Conferences and Computers and Information in Engineering Conference*. American Society of Mechanical Engineers, 2009, pp. 595–601.

[8] A. S. Laliberte, J. E. Herrick, A. Rango, and C. Winters, "Acquisition, orthorectification, and object-based classification of unmanned aerial vehicle (uav) imagery for rangeland monitoring," *Photogrammetric Engineering & Remote Sensing*, vol. 76, no. 6, pp. 661–672, 2010.

[9] J. Larrauri, G. Sorrosal, and M. Gonzlez, "Automatic system for overhead power line inspection using an unmanned aerial vehicle x2014; relifo project," in *Unmanned Aircraft Systems (ICUAS), 2013 International Conference on*, May 2013, pp. 244–252.

[10] W. E. Roper and S. Dutta, "Remote sensing and gis applications for pipeline security assessment," in *2005 ESRI User Conference Proceedings*, vol. 15, 2005.

[11] R. Dobson, C. Brooks, C. Roussi, and T. Colling, "Developing an unpaved road assessment system for practical deployment with high-resolution optical data collection using a helicopter uav," in *Unmanned Aircraft Systems (ICUAS), 2013 International Conference on*, May 2013, pp. 235–243.

[12] C. Zhang, "An uav-based photogrammetric mapping system for road condition assessment," *Int. Arch. Photogramm. Remote Sens. Spatial Inf. Sci*, vol. 37, pp. 627–632, 2008.

[13] H. Bendea, P. Boccardo, S. Dequal, F. Giulio Tonolo, D. Marenchino, and M. Piras, "Low cost uav for post-disaster assessment," *The International Archives of the Photogrammetry, Remote Sensing and Spatial Information Sciences*, vol. 37, no. Part B, pp. 1373–1379, 2008.

[14] T. Suzuki, D. Miyoshi, J.-i. Meguro, Y. Amano, T. Hashizume, K. Sato, and J.-i. Takiguchi, "Real-time hazard map generation using small unmanned aerial vehicle," in *SICE Annual Conference, 2008*. IEEE, 2008, pp. 443–446.

[15] R. Hirokawa, D. Kubo, S. Suzuki, J.-i. Meguro, and T. Suzuki, "A small uav for immediate hazard map generation," in *AIAA Infotech@ Aerospace Conf*, 2007.

[16] S. N. Goward, B. Markham, D. G. Dye, W. Dulaney, and J. Yang, "Normalized difference vegetation index measurements from the advanced very high resolution radiometer," *Remote sensing of environment*, vol. 35, no. 2, pp. 257–277, 1991.

[17] S. A. Shearer and R. Holmes, "Plant identification using color co-occurrence matrices," *Transactions of the ASAE*, vol. 33, no. 6, pp. 1237–1244, 1990.